



Research Article

# Effect of hall current on propagation of plane wave in transversely isotropic thermoelastic medium with two temperature and fractional order heat transfer

Iqbal Kaur<sup>1</sup>  · Parveen Lata<sup>1</sup>

© Springer Nature Switzerland AG 2019

## Abstract

This research is devoted to the study of plane wave propagation in homogeneous transversely isotropic magneto-thermoelastic rotating medium with combined effect of hall current and two temperature. The research is applied to fractional order theory with three-phase lag heat transfer. It is analysed that, for 2-D assumed model, three types of coupled longitudinal waves (quasi-longitudinal, quasi-transverse and quasi-thermal) are present. The wave characteristics like phase velocity, specific loss, attenuation coefficients, energy ratios, penetration depths and amplitude ratios of transmitted and reflected waves are computed numerically and illustrated graphically. The impact of hall current parameter by taking different values is represented graphically. Some particular cases are also derived from this research.

**Keywords** Transversely isotropic · Magneto-thermoelastic · Rotation · Fractional order heat transfer · Hall current · Two temperature · Plane wave propagation

**Mathematics Subject Classification** 74C05 · 74BXX · 80A20 · 74F10

## List of symbols

$\delta_{ij}$	Kronecker delta	$\Omega$	Angular velocity of the solid and equal to $\Omega \mathbf{n}$ , where $\mathbf{n}$ is a unit vector
$C_{ijkl}$	Elastic parameters	$\vec{u}$	Displacement vector
$\beta_{ij}$	Thermal elastic coupling tensor	$\vec{H}_0$	Magnetic field intensity vector
$T$	Absolute temperature	$\vec{j}$	Current density vector
$T_0$	Reference temperature	$F_i$	Components of Lorentz force
$\varphi$	Conductive temperature	$\tau_0$	Relaxation time
$t_{ij}$	Stress tensors	$\epsilon_0$	Electric permeability
$e_{ij}$	Strain tensors	$\delta(t)$	Dirac's delta function
$u_i$	Components of displacement	$\tau_t$	Phase lag of heat flux
$\rho$	Medium density	$\tau_v$	Phase lag of temperature gradient
$C_E$	Specific heat	$\tau_q$	Phase lag of thermal displacement
$a_{ij}$	Two temperature parameters	$\alpha$	Fractional order derivative
$\alpha_{ij}$	Linear thermal expansion coefficient	$\xi$	Wave number
$K_{ij}$	Materialistic constant		
$K_{ij}^*$	Thermal conductivity		
$\omega$	Angular frequency		
$\mu_0$	Magnetic permeability		

✉ Iqbal Kaur, bawahanda@gmail.com; Parveen Lata, parveenlata@pbi.ac.in | <sup>1</sup>Department of Basic and Applied Sciences, Punjabi University, Patiala, Punjab, India.



SN Applied Sciences (2019) 1:900 | <https://doi.org/10.1007/s42452-019-0942-1>

Received: 11 May 2019 / Accepted: 17 July 2019 / Published online: 23 July 2019

## 1 Introduction

The medium deformed due to thermal shock and application of the magnetic field, produces an induced magnetic and electric field in the media. These magnetic and electric field produce the voltage (known as Hall voltage) across conductor. The composite material such as a magneto-thermoelastic material gained considerable importance since last decade because these materials show the required coupling effect between magnetic and electric fields. Study of plane wave propagation in a thermoelastic solids gained considerable importance because of its applications in the area of inspecting materials, magnetometers, geophysics, nuclear fields and related topics. In last decade significant attention has been given in the area of plane wave propagation in thermoelastic and magneto-thermoelastic (MT) medium.

Borejko [1] deliberated the coefficients of transmission and reflection for 3D plane waves in elastic media. Sinha and Elsibai [2] discoursed the refraction and reflection of thermoelastic waves with two relaxation times at the boundary of two semi-infinite media. Ting [3] explored propagation of surface wave in an anisotropic rotating media. Othman and Song [4, 5] presented different hypotheses about magnetothermoelastic waves in homogeneous isotropic medium. Kumar and Chawla [6] discussed the plane wave propagation in anisotropic two and three phase lag (TPL) model. Deswal and Kalkal [7] discussed the problem in a surface suffering a time dependent thermal shock for thermo-viscoelastic interactions in a 3-D homogeneous isotropic media.

The reflection of plane periodic wave's occurrence in thermoelastic micropolar homogeneous transversely isotropic (HTI) media had been studied by Kumar and Gupta [8] to find out the complex velocities of the four waves i.e. quasi-longitudinal displacement (qLD), quasi-transverse micro-rotational (qTM), quasi-transverse displacement (qTD) and quasi thermal (qT) waves. Abouelregal [9] had investigated the induced displacement, temperature, and stress fields in transversely isotropic boundless medium with cylindrical cavity with moving and harmonically heat source with dual phase lag (DPL) model. The effects of reflection and refraction are studied by Gupta [10] at the boundary of elastic and a thermoelastic diffusion media, for plane waves by expanding the Fick law with DPL diffusion model with delay times of both mass flow as well as potential gradient. Beside, Kumar et al. [11] depicted the effect of time, thermal and diffusion phase lags for an axisymmetric heat supply in a ring for DPL model for transfer of heat and diffusion by considering upper and lower surfaces of the ring as friction free.

Youssef [12, 13] proposed a two-temperature model for an elastic half-space with constant elastic parameters

and with generalized thermoelasticity without energy dissipation. Sharma and Kaur [14] had investigated the transverse vibrations due to time varying patch loads in homogeneous thermoelastic thin beams. However, Kumar et al. [15] had explored of uncertainties due to thermo-mechanical sources (concentrated and distributed) using Laplace and Fourier transform technique in a homogeneous transversely isotropic thermoelastic (HTIT) rotating medium with magnetic effect, two temperature and by G–N in presence and absence of energy dissipation w.r.t. thermomechanical sources. Kumar et al. [16] investigated the Rayleigh waves in a MT rotating media in the presence of hall current and two temperature.

Othman et al. [17] proposed a model for generalized magneto-thermoelasticity in an isotropic elastic medium rotated with a uniform angular velocity and with two-temperature and initial stress under LS (Lord–Shulman), GL (Green–Lindsay) and CT (coupled theory) theories of generalized thermoelasticity. Kumar and Kansal [18] found reflected and refracted waves occurrence in MT diffusive half-space medium with voids. Maitya et al. [19] presented plane wave propagation in fibre-reinforced medium with GN–I and II type theories and rotation. Bayones and Abd-Alla [20] discussed 2D problem of thermoelasticity regarding thermoelastic wave propagation in a rotating medium with time-dependent heat source.

Alesemi [21] demonstrated the efficiency of the thermal relaxation time depending upon LS theory, Coriolis and Centrifugal Forces on plane wave's reflection coefficients in an anisotropic MT rotating medium. Despite of this several researchers worked on different theory of thermoelasticity Marin [22–25], Marin and Baleanu [26], Ezzat et al. [27], Marin [28, 29] Ezzat et al. [30], Ezzat et al. [31], Marin and Stan [32], Marin and Nicaise [33], Ezzat and El-Bary [34], Othman and Marin [35], Chauthale et al. [36], Marin [37], Kumar et al. [38], Marin et al. [39], Lata and Kaur [40–42] and Lata and Kaur [43, 44]. In spite of these, not much work has been carried out in study of the plane wave propagation with combined effect of hall current, fractional order TPL heat transfer and two temperature.

In this paper, we have attempted to study the plane wave propagation with combined effect of hall current, fractional order TPL heat transfer and two temperature in HTI magneto thermo elastic medium.

## 2 Basic equations

Following Kumar et al. [45], the simplified Maxwell's equations for a slowly moving and conducting elastic solid are

$$\text{curl } \vec{h} = \vec{j} + \epsilon_0 \frac{\partial \vec{E}}{\partial t}, \quad (1)$$

$$\text{curl} \vec{E} = -\mu_0 \frac{\partial \vec{h}}{\partial t}, \tag{2}$$

$$\vec{E} = -\mu_0 \left( \frac{\partial \vec{u}}{\partial t} + \vec{H}_0 \right), \tag{3}$$

$$\text{div} \vec{h} = 0. \tag{4}$$

Maxwell stress components [45] are given by

$$t_{ij} = \mu_0 (H_i h_j + H_j h_i - H_k h_k \delta_{ij}). \tag{5}$$

The constitutive relations for a HTIT medium are given by

$$t_{ij} = C_{ijkl} e_{kl} - \beta_{ij} T. \tag{6}$$

Equation of motion as described by Schoenberg and Censor [46] for a HTI medium rotating uniformly with an angular velocity and Lorentz force

$$t_{ijj} + F_i = \rho \{ \ddot{u}_i + (\Omega \times (\Omega \times u))_i + (2\Omega \times \dot{u})_i \}, \tag{7}$$

where  $F_i = \mu_0 (\vec{j} \times \vec{H}_0)_i$  are the components of Lorentz force. The terms  $\Omega \times (\Omega \times u)$  and  $2\Omega \times \dot{u}$  are the centripetal acceleration and Coriolis acceleration due to the time-varying motion respectively.

The Eqs. (1)–(7) are appended by generalized Ohm’s law for finite conductivity and hall current effect [47]:

$$J = \frac{\sigma_0}{1 + m^2} \left( E + \mu_0 \left( \dot{u} \times H - \frac{1}{en_e} J \times H_0 \right) \right). \tag{8}$$

The heat conduction equation

$$K_{ij} \left( 1 + \frac{(\tau_t)^\alpha}{\alpha!} \frac{\partial^\alpha}{\partial t^\alpha} \right) \dot{\varphi}_{ji} + K_{ij}^* \left( 1 + \frac{(\tau_v)^\alpha}{\alpha!} \frac{\partial^\alpha}{\partial t^\alpha} \right) \varphi_{ji} = \left( 1 + \frac{(\tau_q)^\alpha}{\alpha!} \frac{\partial^\alpha}{\partial t^\alpha} + \frac{(\tau_q)^{2\alpha}}{2\alpha!} \frac{\partial^{2\alpha}}{\partial t^{2\alpha}} \right) [\rho C_E \ddot{T} + \beta_{ij} T_0 \ddot{e}_{ij}], \tag{9}$$

where  $\beta_{ij} = C_{ijkl} \alpha_{ij}$ ,

$$e_{ij} = \frac{1}{2} (u_{i,j} + u_{j,i}), \quad i, j = 1, 2, 3. \tag{10}$$

$$T = \varphi - a_{ij} \varphi_{,ij},$$

$\beta_{ij} = \beta_i \delta_{ij}, K_{ij} = K_i \delta_{ij}, K_{ij}^* = K_i^* \delta_{ij}$   $i$  is not summed.

Here  $C_{ijkl}$  ( $C_{ijkl} = C_{klij} = C_{jikl} = C_{jilk}$ ) are elastic parameters and having symmetry ( $C_{ijkl} = C_{klij} = C_{jikl} = C_{jilk}$ ). The basis of these symmetries of  $C_{ijkl}$  is due to

1. The stress tensor is symmetric, which is only possible if ( $C_{ijkl} = C_{jilk}$ )

2. If a strain energy density exists for the material, the elastic stiffness tensor must satisfy  $C_{ijkl} = C_{klij}$
3. From stress tensor and elastic stiffness tensor symmetries infer ( $C_{ijkl} = C_{ijlk}$ ) and  $C_{ijkl} = C_{klij} = C_{jikl} = C_{jilk}$

### 3 Formulation and solution of the problem

We consider a perfectly conducting HTI magnetothermoelastic rotating medium with an angular velocity  $\Omega$  and two temperature and TPL fractional order model of generalized thermoelasticity initially at a uniform temperature  $T_0$ , with an initial magnetic field  $\vec{H}_0 = (0, H_0, 0)$  acting towards  $y$  axis. The rectangular Cartesian co-ordinate system  $(x, y, z)$  having origin on the surface ( $z=0$ ) with  $z$  axis directing vertically downwards into the medium is used. For 2-D problem in  $xz$ —plane, we consider

$$u = (u, 0, w).$$

In addition, we consider that

$$E = 0, \Omega = (0, \Omega, 0).$$

From the generalized Ohm’s law

$$J_2 = 0. \tag{11}$$

The  $J_1$  and  $J_3$  using (8) are given as

$$J_1 = \frac{\sigma_0 \mu_0 H_0}{1 + m^2} \left( m \frac{\partial u}{\partial t} - \frac{\partial w}{\partial t} \right), \tag{12}$$

$$J_3 = \frac{\sigma_0 \mu_0 H_0}{1 + m^2} \left( \frac{\partial u}{\partial t} + m \frac{\partial w}{\partial t} \right). \tag{13}$$

Now using the transformation on Eqs. (7)–(9) following Slaughter [48] are as under:

$$C_{11} \frac{\partial^2 u}{\partial x^2} + C_{13} \frac{\partial^2 w}{\partial x \partial z} + C_{44} \left( \frac{\partial^2 u}{\partial z^2} + \frac{\partial^2 w}{\partial x \partial z} \right) - \beta_1 \frac{\partial}{\partial x} \left\{ \varphi - \left( a_1 \frac{\partial^2 \varphi}{\partial x^2} + a_3 \frac{\partial^2 \varphi}{\partial z^2} \right) \right\} - \mu_0 J_3 H_0 = \rho \left( \frac{\partial^2 u}{\partial t^2} - \Omega^2 u + 2\Omega \frac{\partial w}{\partial t} \right), \tag{14}$$

$$(C_{13} + C_{44}) \frac{\partial^2 u}{\partial x \partial z} + C_{44} \frac{\partial^2 w}{\partial x^2} + C_{33} \frac{\partial^2 w}{\partial z^2} - \beta_3 \frac{\partial}{\partial z} \left\{ \varphi - \left( a_1 \frac{\partial^2 \varphi}{\partial x^2} + a_3 \frac{\partial^2 \varphi}{\partial z^2} \right) \right\} - \mu_0 J_1 H_0 = \rho \left( \frac{\partial^2 w}{\partial t^2} - \Omega^2 w - 2\Omega \frac{\partial u}{\partial t} \right), \tag{15}$$

$$\begin{aligned}
 &K_1 \left( 1 + \frac{(\tau_t)^\alpha}{\alpha!} \frac{\partial^\alpha}{\partial t^\alpha} \right) \frac{\partial^2 \varphi}{\partial x^2} + K_3 \left( 1 + \frac{(\tau_t)^\alpha}{\alpha!} \frac{\partial^\alpha}{\partial t^\alpha} \right) \frac{\partial^2 \varphi}{\partial z^2} \\
 &+ K_1^* \left( 1 + \frac{(\tau_v)^\alpha}{\alpha!} \frac{\partial^\alpha}{\partial t^\alpha} \right) \frac{\partial^2 \varphi}{\partial x^2} + K_3^* \left( 1 + \frac{(\tau_v)^\alpha}{\alpha!} \frac{\partial^\alpha}{\partial t^\alpha} \right) \frac{\partial^2 \varphi}{\partial z^2} \\
 &= \left( 1 + \frac{(\tau_q)^\alpha}{\alpha!} \frac{\partial^\alpha}{\partial t^\alpha} + \frac{(\tau_q)^{2\alpha}}{2\alpha!} \frac{\partial^{2\alpha}}{\partial t^{2\alpha}} \right) \\
 &\left[ \rho C_E \frac{\partial^2}{\partial t^2} \left[ \varphi - a_1 \frac{\partial^2 \varphi}{\partial x^2} - a_3 \frac{\partial^2 \varphi}{\partial z^2} \right] \right. \\
 &\left. + T_0 \left\{ \beta_1 \frac{\partial \ddot{u}}{\partial x} + \beta_1 \frac{\partial \ddot{w}}{\partial z} \right\} \right],
 \end{aligned} \tag{16}$$

and

$$t_{xx} = C_{11}e_{xx} + C_{13}e_{xz} - \beta_1 T, \tag{17}$$

$$t_{zz} = C_{13}e_{xx} + C_{33}e_{zz} - \beta_3 T, \tag{18}$$

$$t_{xz} = 2C_{44}e_{xz}, \tag{19}$$

where

$$T = \varphi - \left( a_1 \frac{\partial^2 \varphi}{\partial x^2} + a_3 \frac{\partial^2 \varphi}{\partial z^2} \right),$$

$$\beta_1 = (C_{11} + C_{12})\alpha_1 + C_{13}\alpha_3,$$

$$\beta_3 = 2C_{13}\alpha_1 + C_{33}.$$

To facilitate the solution, below mentioned dimensionless quantities are used:

$$\begin{aligned}
 x' &= \frac{x}{L}, \quad z' = \frac{z}{L}, \quad u' = \frac{\rho C_1^2}{L\beta_1 T_0} u, \\
 w' &= \frac{\rho C_1^2}{L\beta_1 T_0} w, \quad t' = \frac{C_1}{L} t, \quad \Omega' = \frac{L}{C_1} \Omega, \\
 \varphi' &= \frac{\varphi}{T_0}, \quad t'_{xx} = \frac{t_{xx}}{\beta_1 T_0}, \quad t'_{xz} = \frac{t_{xz}}{\beta_1 T_0}, \\
 t'_{zz} &= \frac{t_{zz}}{\beta_1 T_0}, \quad \tau'_T = \frac{C_1}{L} \tau_T, \quad \tau'_v = \frac{C_1}{L} \tau_v, \\
 \tau'_q &= \frac{C_1}{L} \tau_q.
 \end{aligned} \tag{20}$$

Using (20) in Eqs. (14)–(16) and after suppressing the primes, yield

$$\begin{aligned}
 &\frac{\partial^2 u}{\partial x^2} + \delta_1 \frac{\partial^2 w}{\partial x \partial z} + \delta_2 \frac{\partial^2 u}{\partial z^2} - \frac{\partial}{\partial x} \left\{ \varphi - \left( a_1 \frac{\partial^2 \varphi}{\partial x^2} + a_3 \frac{\partial^2 \varphi}{\partial z^2} \right) \right\} \\
 &= \frac{M}{1+m^2} \left[ \frac{\partial u}{\partial t} + m \frac{\partial w}{\partial t} \right] + \frac{\partial^2 u}{\partial t^2} - \Omega^2 u + 2\Omega \frac{\partial w}{\partial t},
 \end{aligned} \tag{21}$$

$$\begin{aligned}
 &\delta_1 \frac{\partial^2 u}{\partial x \partial z} + \delta_2 \frac{\partial^2 w}{\partial x^2} + \delta_3 \frac{\partial^2 w}{\partial z^2} - \frac{\beta_3}{\beta_1} \frac{\partial}{\partial z} \left\{ \varphi - \left( a_1 \frac{\partial^2 \varphi}{\partial x^2} + a_3 \frac{\partial^2 \varphi}{\partial z^2} \right) \right\} \\
 &= -\frac{M}{1+m^2} \left[ m \frac{\partial u}{\partial t} - \frac{\partial w}{\partial t} \right] + \frac{\partial^2 w}{\partial t^2} - \Omega^2 w - 2\Omega \frac{\partial u}{\partial t},
 \end{aligned} \tag{22}$$

$$\begin{aligned}
 &\left( 1 + \frac{C_1 (\tau_t)^\alpha}{\alpha! L} \frac{\partial^{\alpha+1}}{\partial t^{\alpha+1}} \right) \left( K_1 \frac{\partial^2 \varphi}{\partial x^2} + K_3 \frac{\partial^2 \varphi}{\partial z^2} \right)_1 \\
 &+ \left( 1 + \frac{(\tau_v)^\alpha}{\alpha!} \frac{\partial^\alpha}{\partial t^\alpha} \right) \left( K_1^* \frac{\partial^2 \varphi}{\partial x^2} + K_3^* \frac{\partial^2 \varphi}{\partial z^2} \right) \\
 &= \left( 1 + \frac{(\tau_q)^\alpha}{\alpha!} \frac{\partial^\alpha}{\partial t^\alpha} + \frac{(\tau_q)^{2\alpha}}{2\alpha!} \frac{\partial^{2\alpha}}{\partial t^{2\alpha}} \right) \\
 &\left[ \rho C_E \ddot{T} + \frac{\beta_1}{\rho} T_0 \left\{ \beta_1 \frac{\partial \ddot{u}}{\partial x} + \beta_1 \frac{\partial \ddot{w}}{\partial z} \right\} \right],
 \end{aligned} \tag{23}$$

where

$$\delta_1 = \frac{C_{13} + C_{44}}{C_{11}}, \quad \delta_2 = \frac{C_{44}}{C_{11}}, \quad \delta_3 = \frac{C_{33}}{C_{11}}, \quad M = \left( \frac{L\sigma_0 \mu_0^2 H_0^2}{\rho C_1} \right)$$

### 4 Plane wave propagation

We pursue plane wave equations of the form

$$\begin{pmatrix} u \\ w \\ \varphi \end{pmatrix} = \begin{pmatrix} U \\ W \\ \varphi^* \end{pmatrix} e^{i(\omega t - \xi(x \sin \theta - z \cos \theta))}, \tag{24}$$

where  $\sin \theta, \cos \theta$  denotes the projection of wave normal to the x-z plane.

Upon using Eq. (24) in Eqs. (21)–(23) we get

$$\begin{aligned}
 &U [\zeta_1 \xi^2 + \zeta_2] + W [\zeta_3 \xi^2 + \zeta_4] + \varphi^* [\zeta_5 \xi + \zeta_6 \xi^3] = 0, \\
 &U [\zeta_7 \xi^2 + \zeta_8] + W [\zeta_9 \xi^2 + \zeta_{10}] + \varphi^* [\zeta_{11} \xi + \zeta_{12} \xi^3] = 0, \\
 &\zeta_{13} \xi U + \zeta_{14} \xi W + \varphi^* [\zeta_{15} \xi^2 + \zeta_{16}] = 0.
 \end{aligned}$$

and by equating determinant of coefficients of  $U, W$  and  $\varphi^*$  to zero we yields the characteristic equation as

$$A\xi^6 + B\xi^4 + C\xi^2 + D = 0, \tag{25}$$

where

$$\begin{aligned}
 A &= \zeta_{13}\zeta_3\zeta_{12} - \zeta_9\zeta_6\zeta_{13} - \zeta_{14}\zeta_1\zeta_{12} + \zeta_7\zeta_6\zeta_{14} + \zeta_9\zeta_1\zeta_{15} - \zeta_{15}\zeta_7\zeta_3, \\
 B &= \zeta_3\zeta_{13}\zeta_{11} + \zeta_4\zeta_{12}\zeta_{13} - \zeta_9\zeta_5\zeta_{13} - \zeta_{10}\zeta_6\zeta_{13} - \zeta_{14}\zeta_1\zeta_{11} - \zeta_{14}\zeta_2\zeta_{12} + \zeta_{14}\zeta_7\zeta_5 \\
 &\quad + \zeta_6\zeta_8\zeta_{14} + \zeta_{16}\zeta_9\zeta_1 + \zeta_{15}\zeta_9\zeta_2 + \zeta_1\zeta_{10}\zeta_{15} - \zeta_{16}\zeta_3\zeta_7 - \zeta_{15}\zeta_8\zeta_3 - \zeta_{15}\zeta_4\zeta_7, \\
 C &= \zeta_{13}\zeta_4\zeta_{11} - \zeta_5\zeta_{10}\zeta_{13} + \zeta_{14}\zeta_8\zeta_5 + \zeta_{16}\zeta_9\zeta_2 + \zeta_{16}\zeta_1\zeta_{10} + \zeta_{10}\zeta_2\zeta_{15} - \zeta_3\zeta_8\zeta_{16} - \zeta_7\zeta_4\zeta_{16} - \zeta_8\zeta_4\zeta_{15}, \\
 D &= \zeta_2\zeta_{10}\zeta_{16} - \zeta_8\zeta_4\zeta_{16},
 \end{aligned}$$

$$\begin{aligned}
 \zeta_1 &= -\sin^2 \theta - \delta_2 \cos^2 \theta, \\
 \zeta_2 &= \frac{-M}{1+m^2}i\omega + \omega^2 + \Omega^2, \\
 \zeta_3 &= \delta_1 \sin \theta \cos \theta, \\
 \zeta_4 &= \frac{-Mm}{1+m^2}i\omega - 2\omega\Omega i, \\
 \zeta_5 &= i \sin \theta, \\
 \zeta_6 &= ia_1 \sin^3 \theta + ia_3 \sin \theta \cos^2 \theta, \\
 \zeta_7 &= \zeta_3, \\
 \zeta_8 &= \frac{Mm}{1+m^2}i\omega + 2\omega\Omega i, \\
 \zeta_9 &= \delta_2 \sin^2 \theta - \delta_3 \cos^2 \theta, \\
 \zeta_{10} &= \frac{-Mm}{1+m^2}i\omega + \omega^2 + \Omega^2, \\
 \zeta_{11} &= -i \frac{\beta_3}{\beta_1} \cos \theta, \\
 \zeta_{12} &= i \frac{\beta_3}{\beta_1} \cos \theta (a_1 \sin^2 \theta + a_3 \cos^2 \theta), \\
 \zeta_{13} &= -\frac{\beta_1^2}{\rho} T_0 \omega^2 i \sin \theta, \\
 \zeta_{14} &= \frac{\beta_1 \beta_3 T_0 \omega^2 i \cos \theta}{\rho}, \\
 \zeta_{15} &= -\left[ 1 + \frac{C_1}{L} \frac{\tau_T^\alpha}{\alpha!} (i\omega)^{\alpha+1} \right] [K_1 \sin^2 \theta + K_3 \cos^2 \theta] \\
 &\quad - \left[ 1 + \frac{\tau^\alpha}{\alpha!} (i\omega)^\alpha \right] [K_1^* \sin^2 \theta + K_3^* \cos^2 \theta] \\
 &\quad + \left[ 1 + \frac{\tau_q^\alpha}{\alpha!} (i\omega)^\alpha + \frac{\tau_q^{2\alpha}}{2\alpha!} (i\omega)^{2\alpha} \right] \\
 &\quad C_1^2 \rho C_E \omega^2 (a_1 \sin^2 \theta + a_3 \cos^2 \theta), \\
 \zeta_{16} &= \left[ 1 + \frac{\tau_q^\alpha}{\alpha!} (i\omega)^\alpha + \frac{\tau_q^{2\alpha}}{2\alpha!} (i\omega)^{2\alpha} \right] C_1^2 \rho C_E \omega^2.
 \end{aligned}$$

The roots of Eq. (25) give six roots of  $\xi$  that is,  $\pm \xi_1, \pm \xi_2$  and  $\pm \xi_3$ , and we are concerned to the roots with positive imaginary parts. Resultant to these roots, there exists three waves according to descending order of their velocities namely QL, QTS and QT. The phase velocities, attenuation coefficients, specific loss and penetration depth of these waves are obtained by the following expressions.

### 1. Phase velocity

The phase velocities are given by

$$V_i = \frac{\omega}{\text{Re}(\xi_i)}, \quad i = 1, 2, 3$$

where  $V_1, V_2, V_3$  are the velocities of QL, QTS and QT waves respectively (Fig. 1).

### 2. Attenuation coefficient

The attenuation coefficient is defined as

$$Q_i = \text{Im}g(\xi_i), \quad i = 1, 2, 3.$$

where  $Q_1, Q_2, Q_3$  are the attenuation coefficients of QL, QTS and QT waves respectively.

### 3. Specific loss

The specific loss is define as:

$$W_i = \left( \frac{\Delta W}{W} \right) i = 4\pi \left| \frac{\text{Im}g(\xi_i)}{\text{Re}(\xi_i)} \right|, \quad i = 1, 2, 3.$$

where  $W_1, W_2, W_3$  are specific loss of QL, QTS and QT waves respectively.

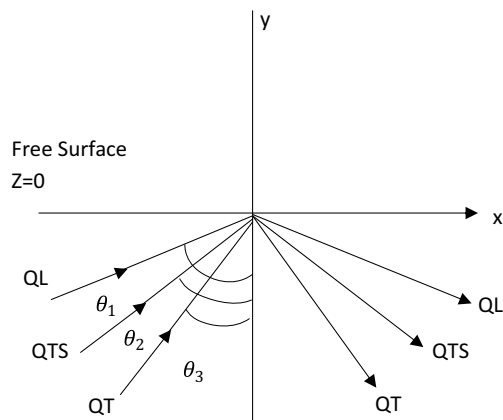


Fig. 1 Geometry of the problem

#### 4. Penetration depth

The penetration depth of plane wave is given by

$$S_i = \frac{1}{\text{Im}g(\xi_i)}, \quad i = 1, 2, 3.$$

where  $S_1, S_2, S_3$  are penetration depth of QL, QTS and QT waves respectively.

### 5 Reflection and transmission at the boundary surfaces

We consider a HTI magneto-thermoelastic half-space occupying the region  $z \geq 0$ . Incident QL, QTS and QT waves at the stress free and thermally insulated surface ( $z=0$ ) will generate reflected QL, QTS and QT waves in the half-space  $z > 0$ . The total displacements, conductive temperature are given by

$$(u, w, \varphi) = \sum_{j=1}^6 (1, d_j, l_j) A_j e^{iM_j}, \tag{26}$$

where

$$M_j = \omega t - \xi_j (x \sin \theta_j - z \cos \theta_j), \quad j = 1, 2, 3,$$

$$M_j = \omega t - \xi_j (x \sin \theta_j + z \cos \theta_j), \quad j = 4, 5, 6.$$

Here subscripts  $j = 1, 2, 3$  respectively denote the quantities corresponding to incident QL, QTS and QT-mode, whereas the subscripts  $j = 4, 5, 6$  denote the corresponding reflected waves,  $\xi_j$  are the roots obtained from Eq. (25).

$$d_j = \frac{\zeta_2 \zeta_{16} + (\zeta_2 \zeta_{15j} - \zeta_{5j} \zeta_{13j} + \zeta_{16} \zeta_{1j}) \xi_j^2 + (\zeta_{1j} \zeta_{15j} - \zeta_{6j} \zeta_{13j}) \xi_j^4}{(\zeta_{9j} \zeta_{15j} - \zeta_{12j}) \xi_j^4 + (\zeta_{10} \zeta_{15j} + \zeta_{9j} \zeta_{16} - \zeta_{11j} \zeta_{14j}) \xi_j^2 - \zeta_{10} \zeta_{16}}, \quad j = 1, 2, 3.$$

$$l_j = \frac{(\zeta_2 \zeta_{10} - \zeta_4 \zeta_8) + (\zeta_{10} \zeta_{1j} + \zeta_2 \zeta_{9j} - \zeta_4 \zeta_{7j} + \zeta_8 \zeta_{3j}) \xi_j^2 + (\zeta_{1j} \zeta_{9j} - \zeta_{3j} \zeta_{7j}) \xi_j^4}{(\zeta_{9j} \zeta_{15j} - \zeta_{12j}) \xi_j^4 + (\zeta_{10} \zeta_{15j} + \zeta_{9j} \zeta_{16} - \zeta_{11j} \zeta_{14j}) \xi_j^2 - \zeta_{10} \zeta_{16}}, \quad j = 1, 2, 3.$$

$$d_j = \frac{\zeta_2 \zeta_{16} + (\zeta_2 \zeta_{15j} - \zeta_{5j} \zeta_{13j} + \zeta_{16} \zeta_{1j}) \xi_j^2 + (\zeta_{1j} \zeta_{15j} - \zeta_{6j} \zeta_{13j}) \xi_j^4}{(\zeta_{9j} \zeta_{15j} - \zeta_{12j}) \xi_j^4 + (\zeta_{10} \zeta_{15j} + \zeta_{9j} \zeta_{16} - \zeta_{11j} \zeta_{14j}) \xi_j^2 - \zeta_{10} \zeta_{16}}, \quad j = 4, 5, 6.$$

$$l_j = \frac{(\zeta_2 \zeta_{10} - \zeta_4 \zeta_8) + (\zeta_{10} \zeta_{1j} + \zeta_2 \zeta_{9j} - \zeta_4 \zeta_{7j} + \zeta_8 \zeta_{3j}) \xi_j^2 + (\zeta_{1j} \zeta_{9j} - \zeta_{3j} \zeta_{7j}) \xi_j^4}{(\zeta_{9j} \zeta_{15j} - \zeta_{12j}) \xi_j^4 + (\zeta_{10} \zeta_{15j} + \zeta_{9j} \zeta_{16} - \zeta_{11j} \zeta_{14j}) \xi_j^2 - \zeta_{10} \zeta_{16}}, \quad j = 4, 5, 6.$$

### 6 Boundary conditions

The dimensionless boundary conditions at the free surface  $z=0$ , are given by

$$t_{33} = 0, \tag{27}$$

$$t_{31} = 0, \tag{28}$$

$$\frac{\partial \varphi}{\partial z} = 0. \tag{29}$$

Using Eq. (26) into the Eqs. (27)–(29), we obtain

$$\sum_{j=1}^3 A_j e^{i(\omega t - \xi_j(x \sin \theta_j))} [-C_{13} i \xi_j \sin \theta_j + C_{33} i d_j \xi_j \cos \theta_j - \beta_3 l_j] - \sum_{j=4}^6 A_j e^{i(\omega t - \xi_j(x \sin \theta_j))} [C_{13} i \xi_j \sin \theta_j + C_{33} i d_j \xi_j \cos \theta_j + \beta_3 l_j] = 0, \tag{30}$$

$$\sum_{j=1}^3 A_j e^{i(\omega t - \xi_j(x \sin \theta_j))} [\xi_j \cos \theta_j - d_j \xi_j \sin \theta_j] - \sum_{j=4}^6 A_j e^{i(\omega t - \xi_j(x \sin \theta_j))} [\xi_j \cos \theta_j + d_j \xi_j \sin \theta_j] = 0, \tag{31}$$

$$\sum_{j=1}^3 A_j e^{i(\omega t - \xi_j(x \sin \theta_j))} [i l_j \xi_j \cos \theta_j] - \sum_{j=4}^6 A_j e^{i(\omega t - \xi_j(x \sin \theta_j))} [i l_j \xi_j \cos \theta_j] = 0. \tag{32}$$

The Eqs. (30)–(32) are satisfied for all values of  $x$ , therefore we have

$$M_1(x, 0) = M_2(x, 0) = M_3(x, 0) = M_4(x, 0) = M_5(x, 0) = M_6(x, 0). \tag{33}$$

From Eqs. (26) and (33), we obtain

$$\xi_1 \sin \theta_1 = \xi_2 \sin \theta_2 = \xi_3 \sin \theta_3 = \xi_4 \sin \theta_4 = \xi_5 \sin \theta_5 = \xi_6 \sin \theta_6. \tag{34}$$

The Eqs. (30)–(32) and (34) yield

$$\sum_{p=1}^3 X_{ip} A_p + \sum_{j=4}^6 X_{ij} A_j = 0, \quad (i = 1, 2, 3), \tag{35}$$

where for  $p = 1, 2, 3$  we have,

$$X_{1p} = \frac{-C_{13}}{\rho C_1^2} i \xi_p \sin \theta_p + \frac{C_{33}}{\rho C_1^2} i d_p \xi_p \cos \theta_p - \frac{\beta_3}{\beta_1} \left[ 1 - a_1 \xi_p^2 \sin^2 \theta_p - a_3 \xi_p^2 \cos^2 \theta_p \right] l_p, \tag{36}$$

$$X_{2p} = i \xi_p \cos \theta_p - i d_p \xi_p \sin \theta_p, \tag{37}$$

$$X_{3p} = il_p \xi_p \cos \theta_p \tag{38}$$

and for  $j = 4, 5, 6$  we have

$$X_{1j} = \frac{-C_{13}}{\rho C_1^2} i \xi_p \sin \theta_p - \frac{C_{33}}{\rho C_1^2} id_p \xi_p \cos \theta_p - \frac{\beta_3}{\beta_1} \left[ 1 - a_1 \xi_p^2 \sin^2 \theta_p - a_3 \xi_p^2 \cos^2 \theta_p \right] l_p \tag{39}$$

$$X_{2j} = -i \xi_j \cos \theta_j - id_j \xi_j \sin \theta_j \tag{40}$$

$$X_{3j} = -il_j \xi_j \cos \theta_j \tag{41}$$

### 6.1 Incident QL-wave

In case of QL wave, the subscript  $p$  takes only one value, that is  $p=1$ , which means  $A_2 = A_3 = 0$ . Dividing the set of Eqs. (35) throughout by  $A_1$ , by solving with Cramer’s rule we get three homogeneous equations as

$$A_{1i} = \frac{A_{i+3}}{A_1} = \frac{\Delta_i^1}{\Delta} \tag{42}$$

### 6.2 Incident QTS-wave

In case of QTS wave, the subscript  $q$  takes only one value, that is  $q=2$ , which means  $A_1 = A_3 = 0$ . Dividing the set of Eqs. (35) throughout by  $A_2$ , by solving with Cramer’s rule we get three homogeneous equations as

$$A_{2i} = \frac{A_{i+3}}{A_2} = \frac{\Delta_i^2}{\Delta} \tag{43}$$

### 6.3 Incident QT-wave

In case of QT wave, the subscript  $q$  takes only one value, that is  $q=3$ , which means  $A_2 = A_1 = 0$ . Dividing the set of Eq. (35) throughout by  $A_3$ , by solving with Cramer’s rule we get three homogeneous equations as

$$A_{3i} = \frac{A_{i+3}}{A_3} = \frac{\Delta_i^3}{\Delta} \tag{44}$$

where  $Z_i (i = 1, 2, 3)$  are the amplitude ratios of the reflected QL, QTS, QT -waves to that of the incident QL-(QTS or QT) waves respectively. Here

$$\Delta = \left| A_{i(i+3)} \right|_{3 \times 3} \tag{45}$$

$$\Delta_i^p, (i = 1, 2, 3) \tag{46}$$

can be obtained by replacing, respectively, the 1st, 2nd and 3rd columns of  $\Delta$  by  $[-X_{1p}, -X_{2p}, -X_{3p}]'$

The energy flux across the surface element is represented as

$$P^* = t_{im} n_m \dot{u}_i \tag{47}$$

where  $n_m$  are the direction cosines of the unit normal and  $\dot{u}_i$  are the components of the particle velocity.

The time average  $P^*$ , is the average energy transmission per unit surface area per unit time and is given at the interface  $z = 0$  as

$$\langle P^* \rangle = \langle \text{Re}(t_{13}) \cdot \text{Re}(\dot{u}_1) + \text{Re}(t_{33}) \cdot \text{Re}(\dot{u}_3) \rangle \tag{48}$$

For complex functions  $a$  and  $b$ , we take

$$\langle \text{Re}(a) \rangle \langle \text{Re}(b) \rangle = \frac{1}{2} \text{Re}(a\bar{b}) \tag{49}$$

The energy ratios  $E_i (i = 1, 2, 3)$  expressions for reflected QL, QT, QTH-wave are given as

1. QL- wave

$$E_{1i} = \frac{\langle P_{i+3}^* \rangle}{\langle P_1^* \rangle}, \quad i = 1, 2, 3. \tag{50}$$

2. QTS- wave

$$E_{1i} = \frac{\langle P_{i+3}^* \rangle}{\langle P_1^* \rangle}, \quad i = 1, 2, 3. \tag{51}$$

3. QT- wave

$$E_{1i} = \frac{\langle P_{i+3}^* \rangle}{\langle P_1^* \rangle}, \quad i = 1, 2, 3. \tag{52}$$

where  $\langle P_i^* \rangle i = 1, 2, 3$  are corresponding to incident QL, QTS, QT waves respectively and  $\langle P_{i+3}^* \rangle i = 1, 2, 3$  are corresponding to reflected QL, QTS, QT waves respectively.

## 7 Particular cases

1. If  $\alpha = 1$  we obtain results for plane wave propagation in magneto-thermoelastic transversely isotropic solid with rotation, hall effect, with two temperature, and with and without energy dissipation and TPL effects.
2. If  $\alpha = 1$  and  $\tau_T = 0, \tau_v = 0, \tau_q = 0$  and  $K^* \neq 0$  we obtain results for plane wave propagation in magneto-thermoelastic transversely isotropic solid with rotation, hall effect, with two temperature and GN III theory (thermoelasticity with energy dissipation).
3. If  $\alpha = 1, \tau_T = 0, \tau_v = 0, \tau_q = 0$  and  $K^* = 0$  we obtain results for plane wave propagation in magneto-thermoelastic transversely isotropic solid with rotation,

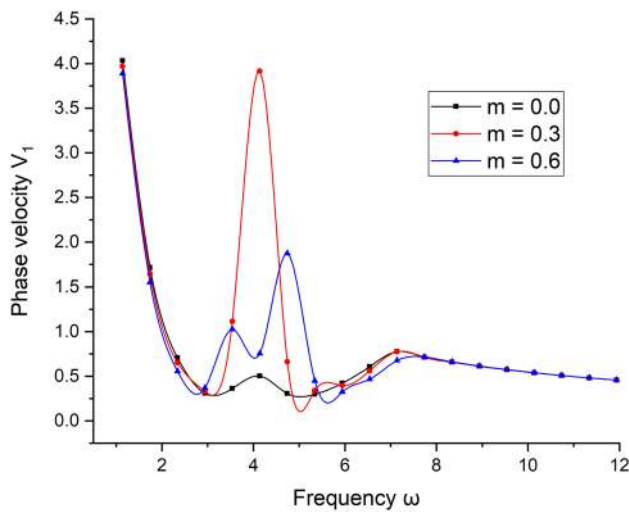


Fig. 2 Variations of phase velocity  $v_1$  with frequency  $\omega$

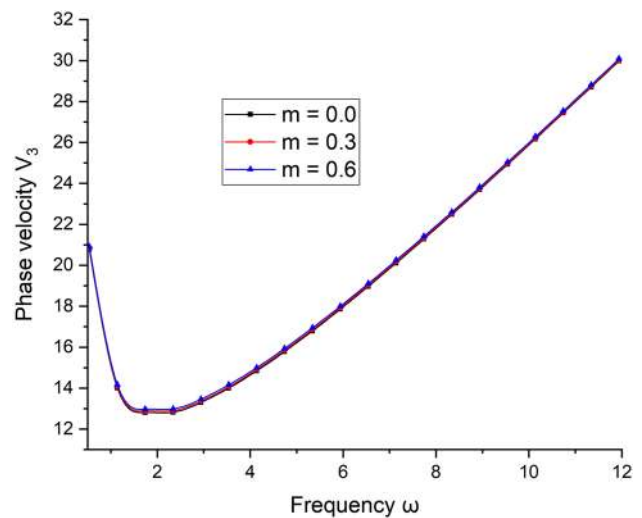


Fig. 4 Variations of phase velocity  $v_3$  with frequency  $\omega$

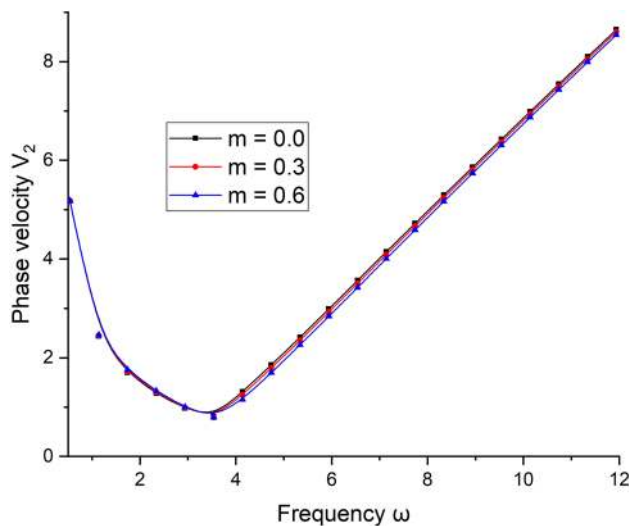


Fig. 3 Variations of phase velocity  $v_2$  with frequency  $\omega$

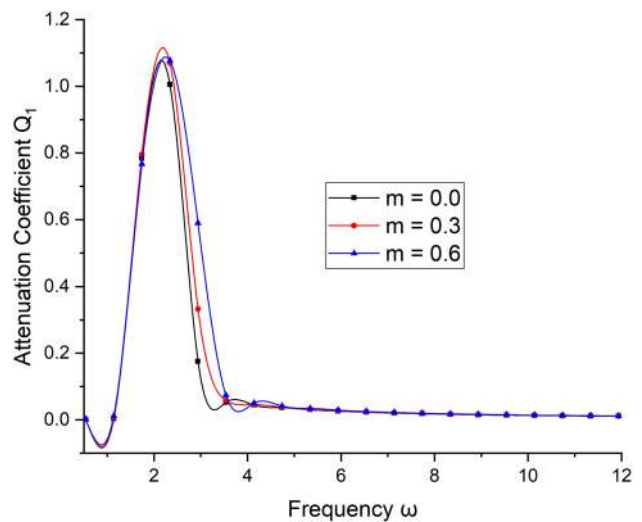


Fig. 5 Variations of attenuation coefficient  $Q_1$  with frequency  $\omega$

hall effect, two temperature and GN II theory (generalized thermoelasticity without energy dissipation).

4. If  $\alpha = 1$  and  $K^* = 0$  we obtain results for plane wave propagation in magneto-thermoelastic transversely isotropic solid with rotation, hall effect, with two temperature and GN II theory with TPL effect
5. If  $\alpha = 1, \tau_T = 0, \tau_v = 0, \tau_q = \tau_0 > 0$  and  $K^* = 0$ , and ignoring  $\tau_q^2$  we obtain results for plane wave propagation in magneto-thermoelastic transversely isotropic solid with rotation, Hall Effect, with two temperature and Lord-Shulman model.

If  $\alpha = 1, \tau_T = 0, \tau_v = 0, \tau_q = 0$  and if the medium is not permeated with the magnetic field i.e.  $\mu_0 = H_0 = 0$  then we obtain results for plane wave propagation in transversely

isotropic thermoelastic solid with rotation, and with two temperature

6. If  $\alpha = 1, C_{11} = C_{33} = \lambda + 2\mu, C_{12} = C_{13} = \lambda, C_{44} = \mu, \alpha_1 = \alpha_3 = \alpha', a_1 = a_3 = a, \beta_1 = \beta_3 = \beta, K_1 = K_3 = K_1^* = K_3^* = K^*$  we obtain expressions for magneto-thermoelastic isotropic materials with rotation, Hall Effect, two temperature and with and without energy dissipation with TPL effect.
7. If  $\alpha = 1, a_1 = a_3 = 0$  we obtain results for magneto-thermoelastic transversely isotropic solid with rotation, Hall Effect, without two temperature, and with and without energy dissipation with TPL effects.



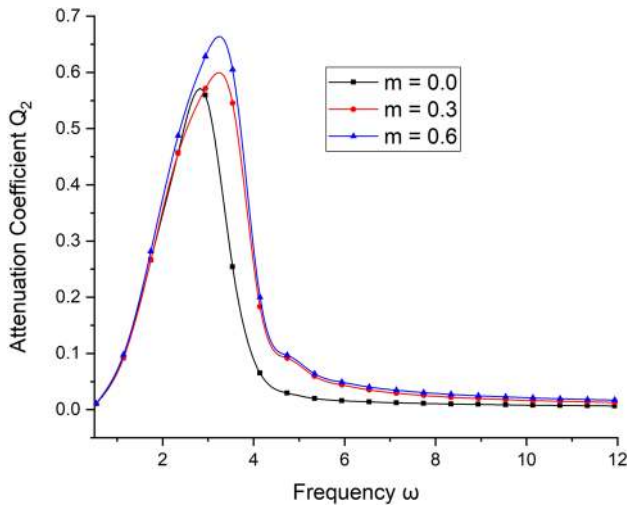


Fig. 6 Variations of attenuation coefficient  $Q_2$  with frequency  $\omega$

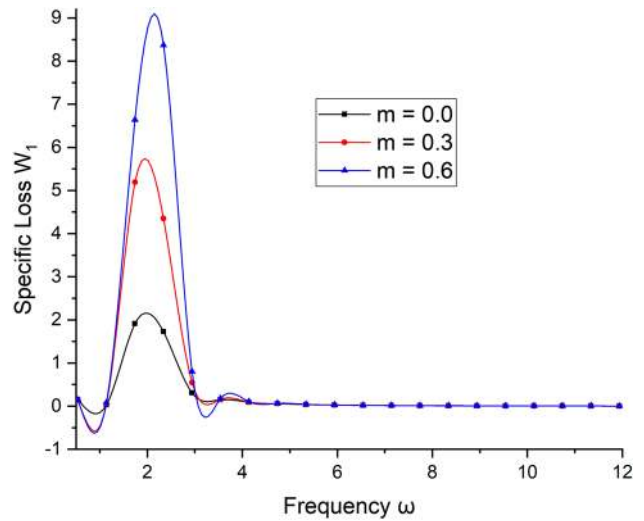


Fig. 8 Variations of specific loss  $W_1$  with frequency  $\omega$

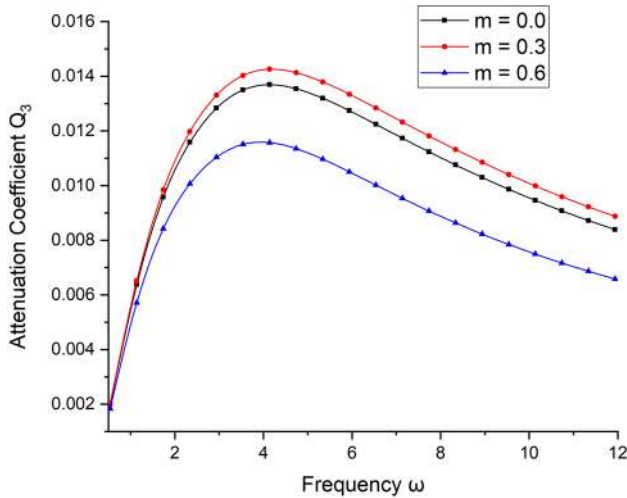


Fig. 7 Variations of attenuation coefficient  $Q_3$  with frequency  $\omega$

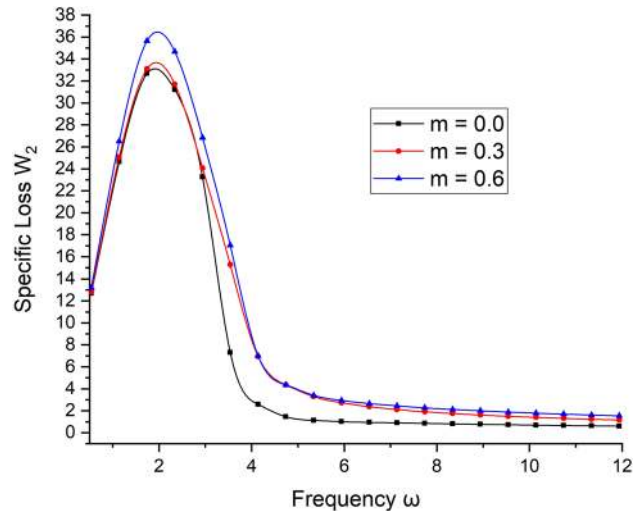


Fig. 9 Variations of specific loss  $W_2$  with frequency  $\omega$

8. If  $\alpha = 1, \Omega = 0$ , then we obtain results for plane wave propagation in transversely isotropic magneto-thermoelastic solid with Hall Effect, with and without energy dissipation, with two temperature and with TPL.

### 8 Numerical results and discussion

To demonstrate the theoretical results and effect of rotation, relaxation time and two temperature, the physical data for cobalt material, which is transversely isotropic, is taken from Dhaliwal and Singh [49] is given as

$$\begin{aligned}
 c_{11} &= 3.07 \times 10^{11} \text{ Nm}^{-2}, & c_{33} &= 3.581 \times 10^{11} \text{ Nm}^{-2}, & c_{13} &= 1.027 \times 10^{10} \text{ Nm}^{-2}, \\
 c_{44} &= 1.510 \times 10^{11} \text{ Nm}^{-2}, & \beta_1 &= 7.04 \times 10^6 \text{ Nm}^{-2} \text{ deg}^{-1}, \\
 \beta_3 &= 6.90 \times 10^6 \text{ Nm}^{-2} \text{ deg}^{-1}, & \rho &= 8.836 \times 10^3 \text{ Kg m}^{-3}, \\
 C_E &= 4.27 \times 10^2 \text{ J Kg}^{-1} \text{ deg}^{-1}, & K_1 &= 0.690 \times 10^2 \text{ Wm}^{-1} \text{ K deg}^{-1}, \\
 K_3 &= 0.690 \times 10^2 \text{ W m}^{-1} \text{ K}^{-1}, & K_1^* &= 1.313 \times 10^2 \text{ W s}, & K_3^* &= 1.54 \times 10^2 \text{ W s}, \\
 T_0 &= 298\text{K}, & H_0 &= 1 \text{ J m}^{-1} \text{ nb}^{-1}, & \epsilon_0 &= 8.838 \times 10^{-12} \text{ Fm}^{-1}, & L &= 1.
 \end{aligned}$$

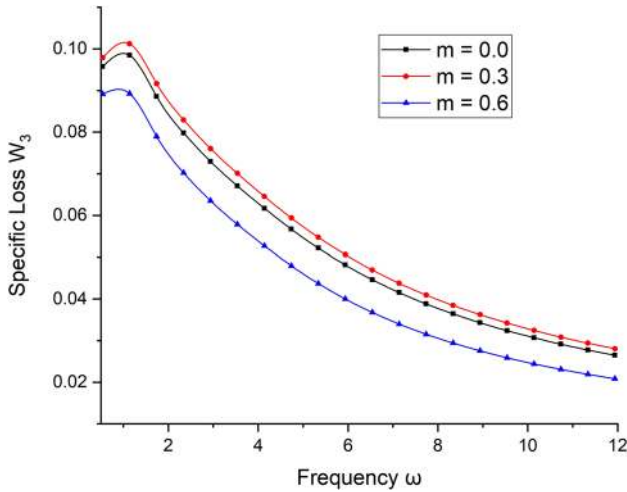


Fig. 10 Variations of specific loss  $W_3$  with frequency  $\omega$

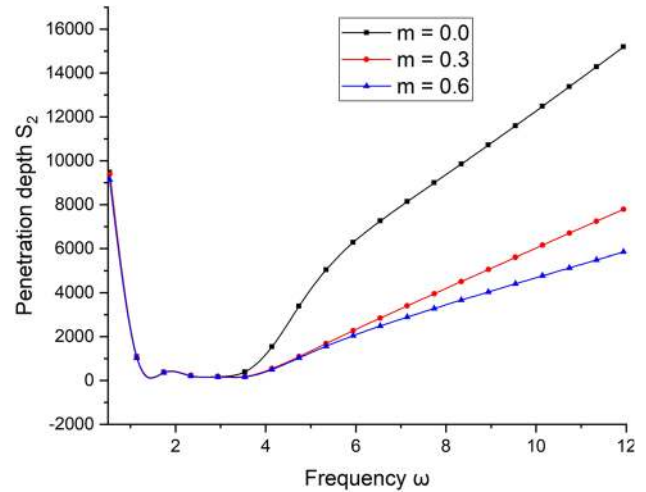


Fig. 12 Variations of penetration depth  $S_2$  with frequency  $\omega$

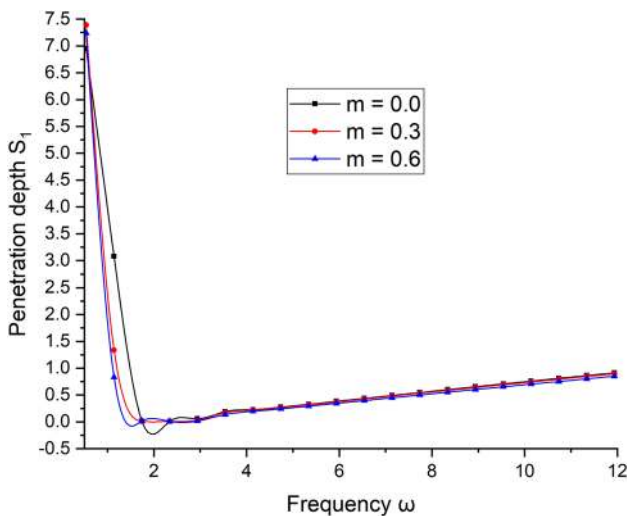


Fig. 11 Variations of penetration depth  $S_1$  with frequency  $\omega$

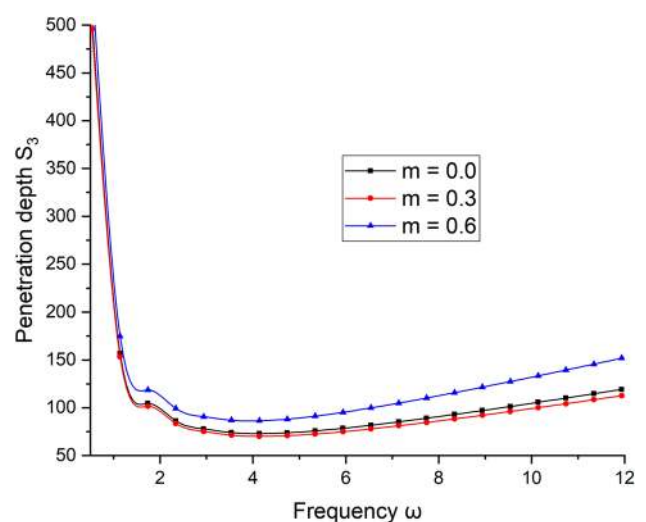


Fig. 13 Variations of penetration depth  $S_3$  with frequency  $\omega$

The values of fractional order parameter  $\alpha$  and two Temperature  $a_1$  and  $a_3$  are taken as 0.5, 0.02, and 0.04 respectively. For the determination of the values of penetration depth, phase velocity, specific loss, attenuation coefficient, amplitude ratios and energy ratios reflected QL, QTS and QT waves w.r.t. incident QL, QTS, and QT waves respectively we have used package MATLAB 8.0.4 and drawn graphically to show the effect of hall current.

1. The line in black colour with square symbol represent  $m = 0.0$ ,
2. The line in red colour with circle symbol represent  $m = 0.3$ ,
3. The line in blue colour with triangle symbol represent  $m = 0.6$ ,

### 8.1 Phase velocity

Figures 2, 3 and 4 indicate the change of phase velocities w.r.t. frequency  $\omega$  respectively. The phase velocity  $V_1$  oscillates in the initial range of the frequency for different value of hall current and remain same in rest of the range. In almost all the frequency range and for all the values of  $m$ , the phase velocity  $V_2, V_3$  follows the same pattern.

### 8.2 Attenuation coefficients

Figures 5, 6 and 7 shows that the values of attenuation w.r.t. frequency respectively. From the graphs it is clear that attenuation coefficient  $Q_1, Q_2$  increases for the initial

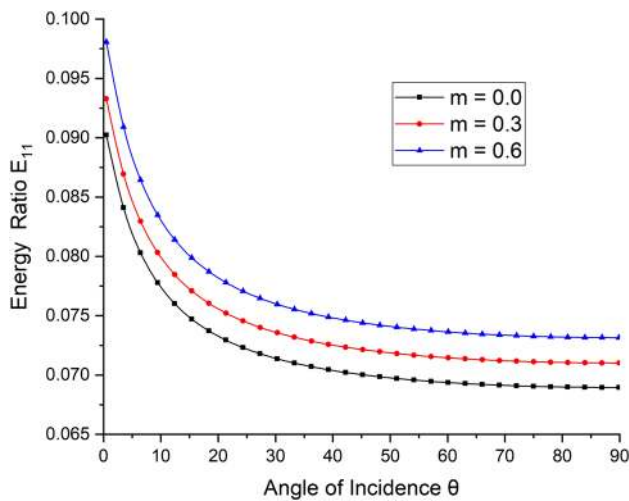


Fig. 14 Variations of energy ratio  $E_{11}$  with angle of incidence  $\theta$

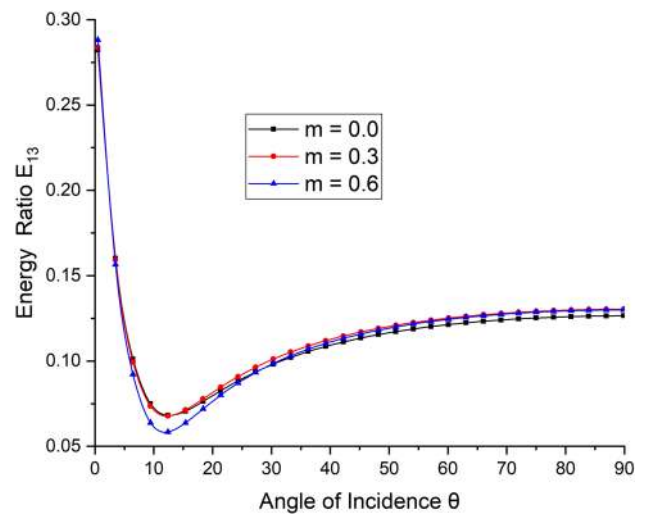


Fig. 16 Variations of energy ratio  $E_{13}$  with angle of incidence  $\theta$

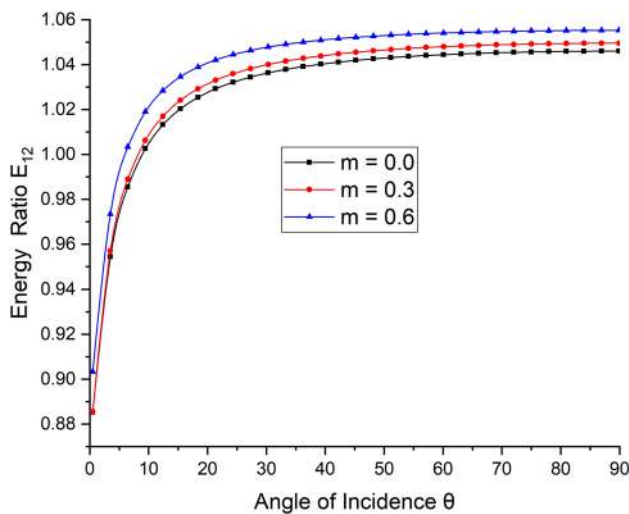


Fig. 15 Variations of energy ratio  $E_{12}$  with angle of incidence  $\theta$

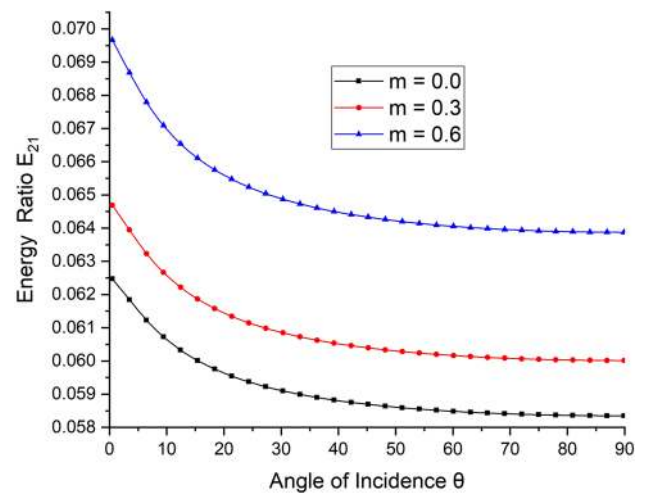


Fig. 17 Variations of energy ratio  $E_{21}$  with angle of incidence  $\theta$

values of the frequencies and then after decreasing the follow the same pattern for all the values of hall current. The value of attenuation coefficient  $Q_3$  increases in the initial range of frequency and have same pattern with different magnitude for different values of hall current.

### 8.3 Specific loss

Figures 8, 9 and 10 exhibits the variations of Specific loss w.r.t. frequency. From the graphs it is clear that the value of specific loss  $W_1$  shows the oscillatory pattern for the initial value of the frequency for all the cases and then shows the same magnitude for rest of the range. The value of specific

loss  $W_2$  shows rise in the initial value of frequency and then after decreasing it comes to steady state for rest of the frequency range in all the cases similar variations. While the value of specific loss  $W_3$  gradually decreases with different magnitudes for all the cases of hall current.

### 8.4 Penetration depth

Figures 11, 12 and 13 shows the variations of penetration depth  $S_1, S_2, S_3$  w.r.t. frequency. Here, we notice a sharp decrease in  $S_2$  and  $S_3$  for all the cases in range  $0.0 \leq \omega \leq 2$ , and the variations approach the boundary surface by increasing slowly and smoothly in the rest.

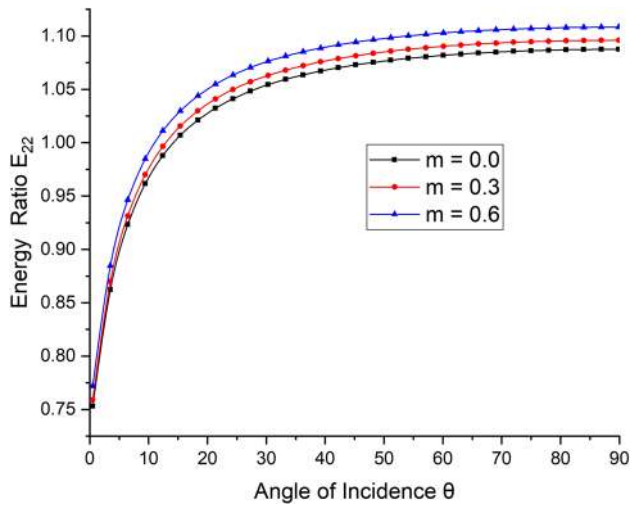


Fig. 18 Variations of energy ratio  $E_{22}$  with angle of incidence  $\theta$

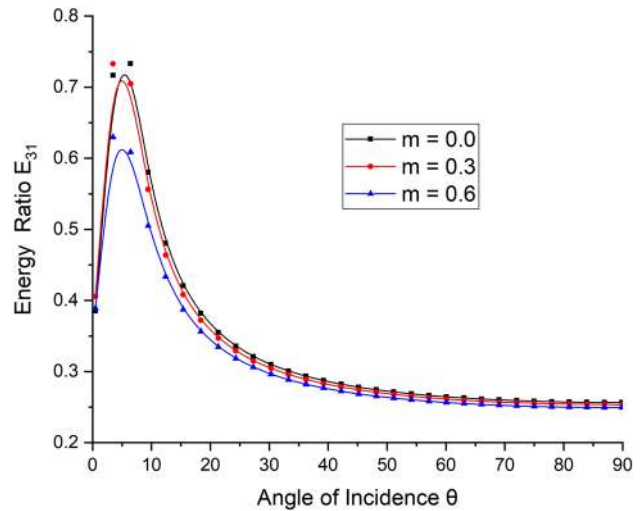


Fig. 20 Variations of energy ratio  $E_{31}$  with angle of incidence  $\theta$

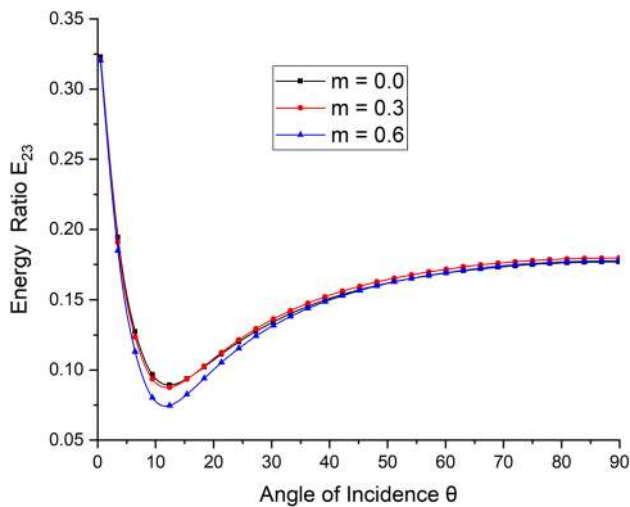


Fig. 19 Variations of energy ratio  $E_{23}$  with angle of incidence  $\theta$

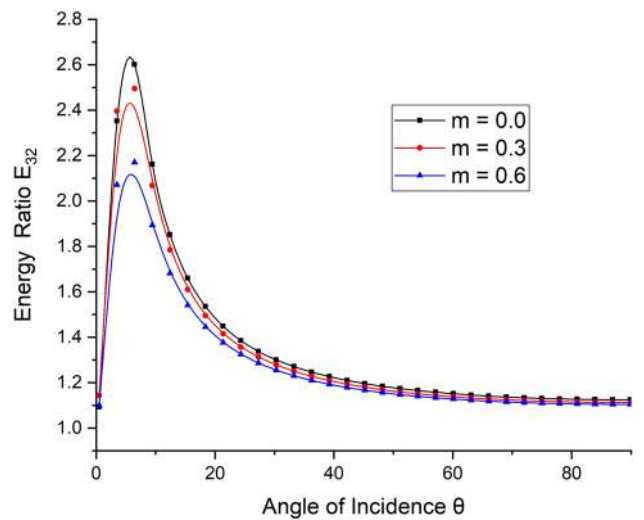


Fig. 21 Variations of energy ratio  $E_{32}$  with angle of incidence  $\theta$

## 8.5 Energyratios

### 8.5.1 Incident QL wave

Figure 14 depicts the change of energy ratio  $E_{11}$  w.r.t. angle of incidence  $\theta$ . It shows that the values of  $E_{11}$  decreases gradually with the change in angle of incidence corresponding

to all the cases of hall current. Figure 15 shows the variations of energy ratio  $E_{12}$  w.r.t. angle of incidence  $\theta$ . Here the value increases and show same increasing pattern but difference in magnitude. Figure 16 depicts the changes of Energy ratio  $E_{13}$  w.r.t. angle of incidence  $\theta$ . It is noticed that the values decreases sharply in the initial range of angle and increase gradually throughout the range.

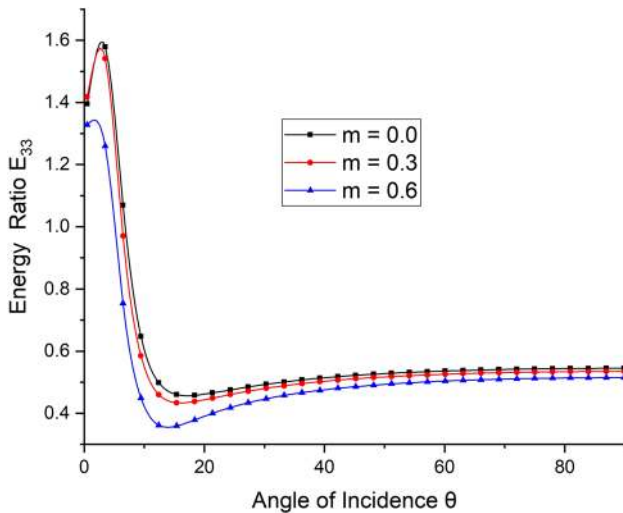


Fig. 22 Variations of energy ratio  $E_{33}$  with angle of incidence  $\theta$

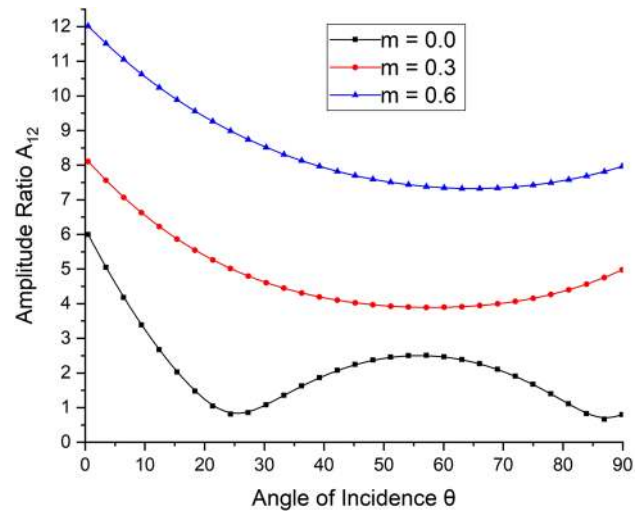


Fig. 24 Variations of amplitude ratio  $A_{12}$  with angle of incidence  $\theta$

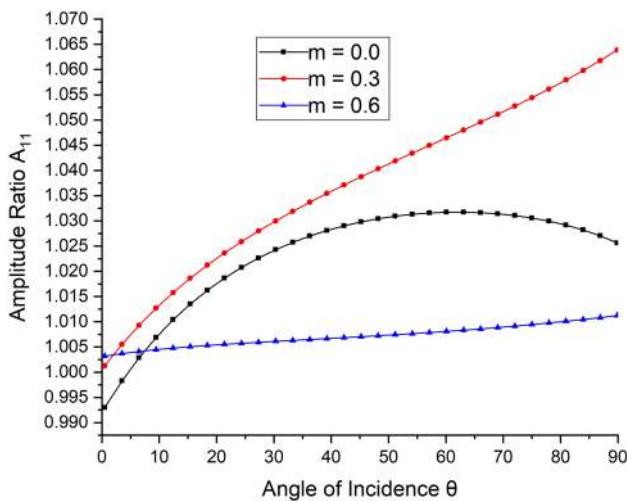


Fig. 23 Variations of amplitude ratio  $A_{11}$  with angle of incidence  $\theta$

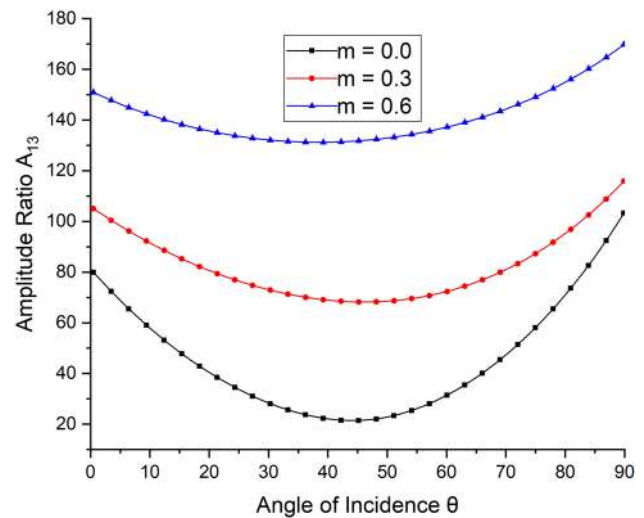


Fig. 25 Variations of amplitude ratio  $A_{13}$  with angle of incidence  $\theta$

### 8.5.2 Incident QTS wave

Figure 17 depicts the change of Energy ratio  $E_{21}$  w.r.t. angle of incidence  $\theta$ . Here corresponding to all the cases, we notice similar decreasing trends with difference in magnitudes for the whole range and show significantly variation for  $m$ . Figure 18 depicts the Variations in  $E_{22}$  w.r.t. angle of incidence  $\theta$ . Here corresponding to all the cases, there is sharp increases in initial range and then shows steady state for rest of range of  $\theta$  Fig. 18. Variations of  $E_{23}$  w.r.t. angle of incidence  $\theta$  are shown in Fig. 19. Here, we notice

values decreases sharply in the initial range of angle and increase gradually throughout the range.

### 8.5.3 Incident QT wave

Figures 20, 21 and 22 depict the Variations of Energy ratios  $E_{31}$ ,  $E_{32}$ ,  $E_{33}$  w.r.t. angle of incidence  $\theta$ . Hereafter sharp increase  $E_{31}$ ,  $E_{32}$  and  $E_{33}$ , with increase in angle of incidence  $\theta$  for all the cases of hall current.

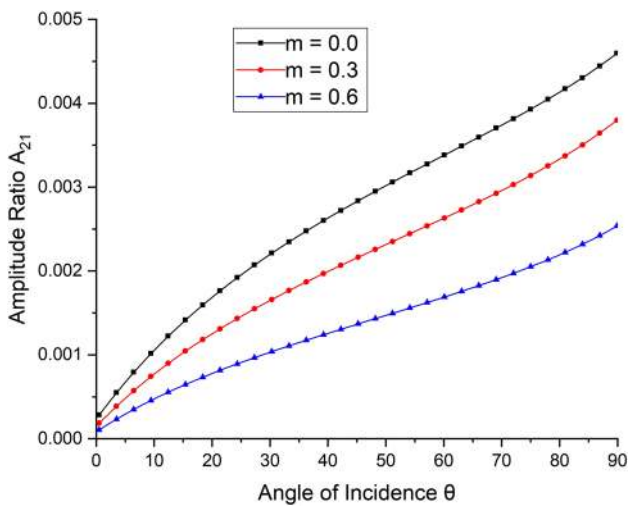


Fig. 26 Variations of amplitude ratio  $A_{21}$  with angle of incidence  $\theta$

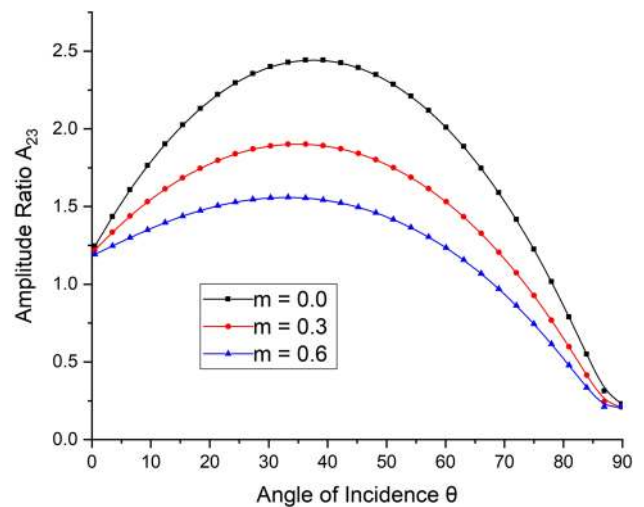


Fig. 28 Variations of amplitude ratio  $A_{23}$  with angle of incidence  $\theta$

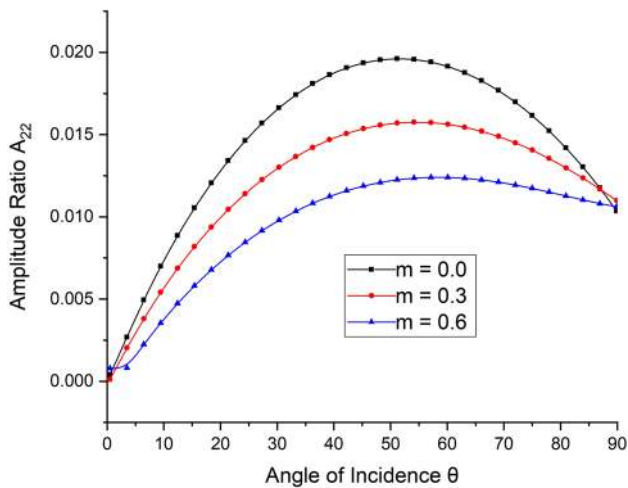


Fig. 27 Variations of amplitude ratio  $A_{22}$  with angle of incidence  $\theta$

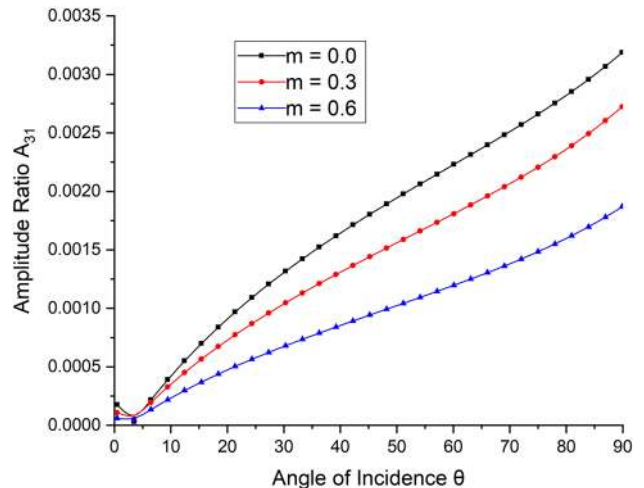


Fig. 29 Variations of amplitude ratio  $A_{31}$  with angle of incidence  $\theta$

## 8.6 Amplitude ratios

### 8.6.1 Incident QL wave

Figures 23, 24 and 25 shows variations of amplitude ratio  $A_{11}$ ,  $A_{12}$ ,  $A_{13}$  w.r.t. angle of incidence  $\theta$ . Here, we notice that, initially, there is linear increase in the values of  $A_{11}$  for  $m = 0.0, 0.3$  while for  $m = 0.6$ , it shows the curve form. The amplitude ratio  $A_{12}$  and  $A_{13}$  shows different pattern for every case of hall current with angle of incidence  $\theta$

### 8.6.2 Incident QTS wave

Figures 26, 27 and 28 depicts the variations of amplitude ratio  $A_{21}$ ,  $A_{22}$ ,  $A_{23}$  w.r.t. angle of incidence  $\theta$ . Here, we notice that a linear increase in amplitude ratios  $A_{21}$  for all the cases of hall current while  $A_{22}$  and  $A_{23}$  shows opposite behaviour for all the cases of  $m$ .

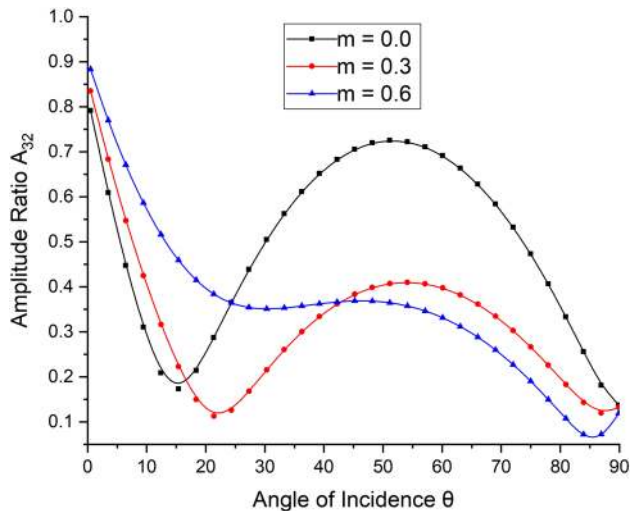


**Fig. 30** Variations of amplitude ratio  $A_{32}$  with angle of incidence  $\theta$

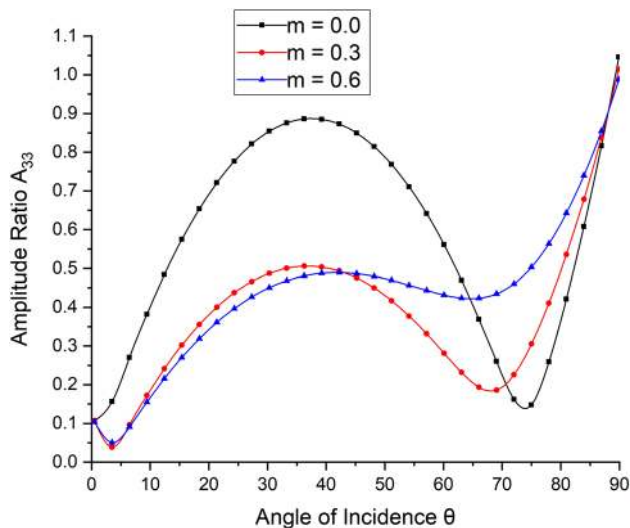


**Fig. 31** Variations of amplitude ratio  $A_{33}$  with angle of incidence  $\theta$

### 8.6.3 Incident QT wave

Figures 29, 30 and 31 show the variations of amplitude ratios  $A_{31}$ ,  $A_{32}$ ,  $A_{33}$  w.r.t. angle of incidence  $\theta$  respectively.. Here, we notice that these variations shows effect of hall effect parameter  $a$  on the amplitude ratios  $A_{31}$ ,  $A_{32}$ ,  $A_{33}$ .

## 9 Conclusions

From the analysis of graphs we conclude

1. The frequency of waves formed in the material have significant effect on the phase velocity, attenuation coefficients, specific loss and penetration depth of various kinds of waves.
2. The magnitude of energy ratios is also effected by the angle of incidence. As angle of incidence increases, we notice less variation in the magnitudes of energy ratios.
3. Hall current and two temperature changes the magnitude of waves. With the increase in the hall current, the magnitude of waves are reduced.
4. The plane waves signals provides information about the inner earth structure and also useful in inspection of materials, magnetometers, geophysics, nuclear fields and related topics.

## Compliance with ethical standards

**Conflict of interest** We have no conflict of interest.

## References

1. Borejko P (1996) Reflection and transmission coefficients for three dimensional plane waves in elastic media. *Wave Motion* 24:371–393
2. Sinha S, Elsibai K (1997) Reflection and refraction of thermoelastic waves at an interface of two semi-infinite media with two relaxation times. *J Therm Stresses* 20:129–145
3. Ting TCT (2004) Surface waves in a rotating anisotropic elastic half-space. *Wave Motion* 40:329–346
4. Othman MIA, Song YQ (2006) The effect of rotation on the reflection of magneto-thermoelastic waves under thermoelasticity without energy dissipation. *Acta Mech* 184:89–204
5. Othman MIA, Song YQ (2008) Reflection of magneto-thermoelastic waves from a rotating elastic half-space. *Int J Eng Sci* 46:459–474
6. Kumar RACV (2011) A study of plane wave propagation in anisotropic threephase-lag model and two-phae-lag model. *Int Commun Heat Mass Transf* 38:1262–1268
7. Deswal S, Kalkal KK (2015) Three-dimensional half-space problem within the framework of two-temperature thermo-viscoelasticity with three-phase-lag effects. *Appl Math Model* 39:7093–7112
8. Kumar R, Gupta RR (2012) Plane waves reflection in micropolar transversely isotropic generalized thermoelastic half-space. *Math Sci* 6(6):1–10
9. Abouelregal AE (2013) Generalized thermoelastic infinite transversely isotropic body with a cylindrical cavity due to moving heat source and harmonically varying heat. *Meccanica* 48:1731–1745
10. Kumar R, Gupta V (2015) Dual-phase-lag model of wave propagation at the interface between elastic and thermoelastic diffusion media. *J Eng Phys Thermophys* 88(1):252–265
11. Kumar R, Sharma N, Lata P (2016) Effects of thermal and diffusion phase-lags in a plate with axisymmetric heat supply. *Multi-discipl Model Mater Struct* 12(2):275–290

12. Youssef HM (2013) State-space approach to two-temperature generalized thermoelasticity without energy dissipation of medium subjected to moving heat source. *Appl Math Mech Engl Ed* 34(1):63–74
13. Youssef HM (2016) Theory of generalized thermoelasticity with fractional order strain. *J Vib Control* 22(18):3840–3857
14. Sharma JN, Kaur R (2015) Modeling and analysis of forced vibrations in transversely isotropic thermoelastic thin beams. *Mechanica* 50:189–205
15. Kumar R, Sharma Nidhi, Lata Parveen (2016) Thermomechanical interactions in transversely isotropic magneto-thermoelastic medium with vacuum and with and without energy dissipation with combined effects of rotation, vacuum and two temperatures. *Appl Math Model* 40(13–14):6560–6575
16. Kuma R, Sharma N, Lata P (2017) Effects of hall current and two temperatures intransversely isotropic magneto-thermoelastic with and without energy dissipation due to ramp-type heat. *Mech Adv Mater Struct* 24(8):625–635
17. Othman MIA, Abo-Dahab SM, Alsebaey ONS (2017) Reflection of plane waves from a rotating magneto-thermoelastic medium with two-temperature and initial stress under three theories. *Mech Mech Eng* 21(2):217–232
18. Kumar R, Kansal T (2017) Reflection and refraction of plane harmonic waves at an interface between elastic solid and magneto-thermoelastic diffusion solid with voids. *Comput Methods Sci Technol* 23(1):43–56
19. Maitya N, Barikb S, Chaudhuri P (2017) Propagation of plane waves in a rotating magneto-thermoelastic fiber-reinforced medium under GN theory. *Appl Comput Mech* 11:47–58
20. Bayones F, Abd-Alla A (2017) Eigenvalue approach to two dimensional coupled magneto-thermoelasticity in a rotating isotropic medium. *Results Phys* 7:2941–2949
21. Alesemi M (2018) Plane waves in magneto-thermoelastic anisotropic medium based on (L–S) theory under the effect of Coriolis and centrifugal forces. In: *International conference on materials engineering and applications*
22. Marin M (1996) Generalized solutions in elasticity of micropolar bodies with voids. *Rev de la Acad Canaria de Ciencias* 8:101–106
23. Marin M (2009) On the minimum principle for dipolar materials with stretch. *Nonlinear Anal Real World Appl* 10(3):1572–1578
24. Marin M (2010) A partition of energy in thermoelasticity of microstretch bodies. *Nonlinear Anal: Real World Appl* 11(4):2436–2447
25. Marin M (1997) Cesaro means in thermoelasticity of dipolar bodies. *Acta Mech* 122(1–4):155–168
26. Marin M, Baleanu D (2016) On vibrations in thermoelasticity without energy dissipation for micropolar bodies. *Bound Value Probl* 2016:111
27. Ezzat MA, El-Karamany AS, Ezzat SM (2012) Two-temperature theory in magneto-thermoelasticity with fractional order dual-phase-lag heat transfer. *Nucl Eng Des* 252:267–277
28. Marin M (1997) On weak solutions in elasticity of dipolar bodies with voids. *J Comput Appl Math* 82(1–2):291–297
29. Marin M (2008) Weak solutions in elasticity of dipolar porous materials. *Math Probl Eng* 2008:1–8
30. Ezzat M, Al-Bary A (2016) Magneto-thermoelastic viscoelastic materials with memory dependent derivatives involving two temperature. *Int J Appl Electromagn Mech* 50(4):549–567
31. Ezzat M, Al-Bary A (2017) Fractional magneto-thermoelastic materials with phase lag Green–Naghdi theories. *Steel Compos Struct* 24(3):297–307
32. Marin M, Stan G (2013) Weak solutions in elasticity of dipolar bodies with stretch. *Carpathian J Math* 29(1):33–40
33. Marin M, Nicaise S (2016) Existence and stability results for thermoelastic dipolar bodies with double porosity. *Continuum Mech Thermodyn* 28(6):1645–1657
34. Ezzat MA, El-Karamany AS, El-Bary AA (2017) Two-temperature theory in Green–Naghdi thermoelasticity with fractional phase-lag heat transfer”. *Microsyst Technol* 24(2):951–961
35. Othman MIA, Marin M (2017) Effect of thermal loading due to laser pulse on thermoelastic porous medium under G-N theory. *Results Phys* 7:3863–3872
36. Chauthale S, Khobragade NW (2017) thermoelastic response of a thick circular plate due to heat generation and its thermal stresses. *Glob J Pure Appl Math* 13:7505–7527
37. Marin M (1998) Contributions on uniqueness in thermoelastodynamics on bodies with voids. *Rev Ciencias Mat* 16(2):101–109
38. Kumar R, Kaushal P, Sharma R (2018) Transversely isotropic magneto-visco thermoelastic medium with vacuum and without energy dissipation. *J Solid Mech* 10(2):416–434
39. Marin M, Ellahi R, Chirilă A (2017) On solutions of Saint-Venant’s problem for elastic dipolar bodies with voids. *Carpathian J Math* 33(2):219–232
40. Lata P, Kaur I (2019) Transversely isotropic thick plate with two temperature and GN type-III in frequency domain. *Coupled Syst Mech* 8(1):55–70
41. Lata P, Kaur I (2019) Study of transversely isotropic thick circular plate due to ring load with two temperature and Green–Naghdi theory of type-I, II and III. In: *International conference on sustainable computing in science, technology and management (SUSCOM-2019)*, Elsevier SSRN., Amity University Rajasthan, Jaipur, India
42. Lata P, Kaur I (2019) Thermomechanical interactions in transversely isotropic thick circular plate with axisymmetric heat supply. *Struct Eng Mech* 69(6):607–614
43. Lata P, Kaur I (2019) Transversely isotropic magneto thermoelastic solid with two temperature and without energy dissipation in generalized thermoelasticity due to inclined load. *SN Appl Sci* 1:426
44. Lata P, Kaur I (2019) Effect of rotation and inclined load on transversely isotropic magneto thermoelastic solid. *Struct Eng Mech* 70(2):245–255
45. Kumar R, Sharma N, Lata P (2016) Thermomechanical interactions in transversely isotropic magneto-thermoelastic medium with vacuum and with and without energy dissipation with combined effects of rotation, vacuum and two temperatures. *Appl Math Model* 40(13–14):6560–6575
46. Schoenberg M, Censo D (1973) Elastic waves in rotating media. *Q Appl Math* 31:115–125
47. Lata P, Kaur I (2018) Effect of hall current in transversely isotropic magneto-thermoelastic rotating medium with fractional order heat transfer due to normal force. *Adv Mater Res* 7(3):203–220
48. Slaughter WS (2002) *The linearized theory of elasticity*. Birkhäuser, Boston
49. Dhaliwal R, Singh A (1980) *Dynamic coupled thermoelasticity*. New Delhi India Hindustan Publication Corporation

**Publisher’s Note** Springer Nature remains neutral with regard to jurisdictional claims in published maps and institutional affiliations.